# Superconducting Integrated Microcircuits Based on NbTiN/Al Transmission Lines Operating at Frequencies Above 1 THz

Nickolay V. Kinev
*Laboratory of Superconducting Devices for Signal Detection and Processing*
*Kotelnikov Institute of Radio Engineering and Electronics of RAS*
Moscow, Russia
nickolay@hitech.cplire.ru

Artem M. Chekushkin
*Laboratory of Superconducting Devices for Signal Detection and Processing*
*Kotelnikov Institute of Radio Engineering and Electronics of RAS*
Moscow, Russia
chekushkin@hitech.cplire.ru

Fedor V. Khan
*Laboratory of Superconducting Devices for Signal Detection and Processing*
*Kotelnikov Institute of Radio Engineering and Electronics of RAS*
Moscow, Russia
khanfv@hitech.cplire.ru

Valery P. Koshelets
*Laboratory of Superconducting Devices for Signal Detection and Processing*
*Kotelnikov Institute of Radio Engineering and Electronics of RAS*
Moscow, Russia
valery@hitech.cplire.ru

2023 Radiation and Scattering of Electromagnetic Waves (RSEMW) | 979-8-3503-2237-8/23/$31.00 ©2023 IEEE | DOI: 10.1109/RSEMW58451.2023.10202053

***Abstract*—The results of the development and testing of superconducting integrated microcircuits based on NbTiN/Al transmission lines at the frequencies up to 1.1 THz are presented. The integrated circuits consist of a slot planar antenna made of thin film of NbTiN coupled to a NbTiN/Al microstrip line, and a superconductor-insulator-superconductor (SIS) junction based on Nb/AlN/NbN operating as a terahertz (THz) detector. Two different designs having the operating range of 0.9-1.2 THz were numerically simulated, fabricated and experimentally tested. A strong pumping of SIS detector by a signal of the backward wave oscillator (BWO) around frequency of 1.05 THz was observed, which demonstrated the applicability of fabricated transmission lines at frequencies higher than 750 GHz, where the traditionally used Nb/Nb transmission lines cannot operate.**

***Keywords—terahertz detection, transmission lines, SIS junctions***

## I. Introduction

Receivers of THz range are demanded in many fields: space and atmospheric research, biomedical applications, communication technologies, as well as for basic research in material science and molecular spectroscopy [1-3]. At the same time, the most sensitive detectors in THz range are SIS junctions due to low operating temperature and strong nonlinearity provided by a quasiparticle tunneling through the barrier [4-5]. For most applications of SIS receivers, the Nb-based superconducting structures ($Nb/AlO_x/Nb$ or Nb/AlN/NbN) operating at liquid helium temperature of 4.2 K are used. Also, some modern tasks require Al-based junctions [6], but extremely low temperature (below 300 mK) is a technical problem. The key task in the development of the highly sensitive receiving system is coupling of the weak input signal to the detecting element, that is solved by means of transmission lines. For the Nb-based SIS junctions, microstrip and coplanar transmission lines made of Nb thin films are traditionally used. The operating frequency of Nb-based lines is limited by about 750 GHz due to sharp increase of losses in the niobium films with frequency increase, according to Mattis-Bardeen theory [7]. This limitation is caused by the fundamental properties of superconducting materials represented by the superconductor energy gap $\Delta$. Hence, more high-frequency transmission lines are required for applications up to 1 THz and higher. The most suitable lines for higher frequency range are NbTiN-based lines having the fundamental frequency limit of about 1.4 THz [8-9].

## II. Experimental Samples

### A. Desings

Two different designs of the integrated circuit containing Nb/AlN/NbN-based SIS junctions implemented into $NbTiN/SiO_2/Al$-based transmission line were developed and numerically simulated. The designs are presented in Fig. 1. Both designs consist of a slot planar antenna in the base circuit electrode of NbTiN, twin SIS junctions each having an area of 1 $\mu m^2$ connected in parallel, and a transmission line matched with the antenna by input and with the junctions by output. Twin SIS junctions are traditionally used for increasing the operating frequency bandwidth of the detector. The design #1 (see Fig. 1(a) on top) implements two detectors embedded in a traditional microstrip lines having lengths $\lambda/4$ (the short section) and $3\lambda/4$ (the long one) to estimate losses in the transmission line by measuring the detected power in different sections. The design #2 (see Fig. 1(b)) contains two symmetric sections with the resonator embedded, which allows to estimate losses in thin film from the quality factor of the resonator. The antenna is identical in both designs #1 and #2. The chip is mounted on the back surface of the silicon lens forming the input quasioptical lens-antenna system, as shown in Fig. 1(a) on bottom. The sample on the lens is placed inside a magnetic shield and cooled to a temperature of 4.2 K in a cryogenic system.

Numerical simulations of the designs were carried out using the microwave 3D-modeling software Ansys™ HFSS. This method allows one to simulate complex structures, treating properly the boundary effects, the distribution of electromagnetic fields and mutual influence of the elements on each other. As there is no any in-built tool to take into account superconducting properties of the materials, we used

The study is supported by the Russian Science Foundation No 23-79-00019, https://rscf.ru/project/23-79-00019/.

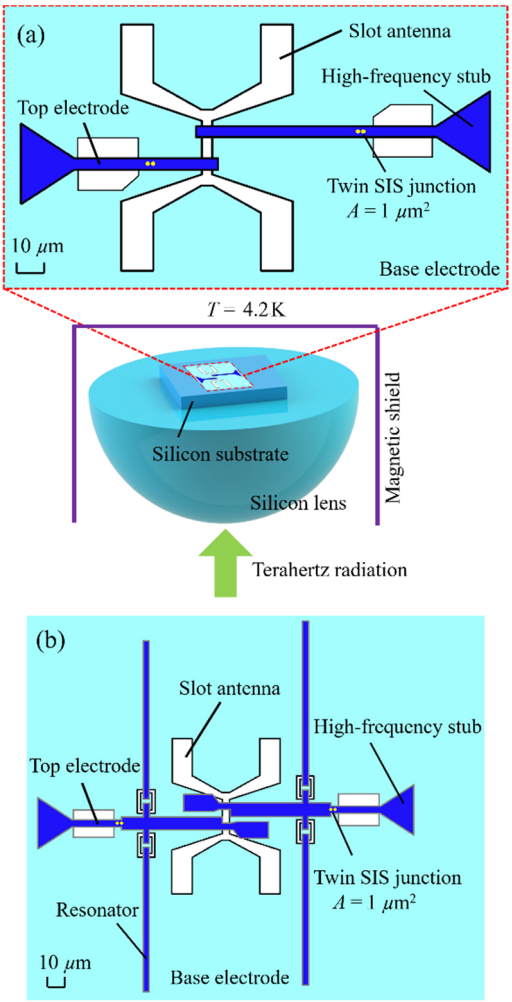


Fig. 1. (a) On top – the layout of the microcircuit (design #1) containing the slot antenna, the twin Nb/AlN/NbN-based SIS junctions and the NbTiN/Al-based microstip line. On bottom – the design of the receiving lens antenna. (b) Layout of the microcircuit (design #2) containing the slot antenna, the twin SIS junctions, the microstip line and the resonators, all based on the same materials as in design #1.

the method proposed in [10-11]. First, we generated datasets for surface impedance of superconducting films using the expressions of Mattis-Bardeen theory [7]. Parameters of the NbTiN film were taken from recent time-domain spectroscopy measurements [12]. Second, we implemented the datasets into Ansys HFSS and assigned boundary conditions on the surfaces of superconducting electrodes.

The impedance of the SIS junction $Z_{SIS}$ in the model consists of the normal-state resistance of the junction $R_n$ and its capacitance $C$ connected in parallel, which can be introduced in simulation by "*Lumped RLC*" boundary condition. All the junctions were treated as serially connected *Lumped RLC* and lumped port with the resistance $R_{port} = 1$ mΩ, which is much less than Re($Z_{SIS}$). Since there are two SIS junctions on a distance of around 2 $\mu$m between each other, they were modeled as separate objects as shown in Fig. 2. In order to obtain the total power absorbed on the SIS junctions $P_a$ (dB) from calculated $S_{21}$ parameters we used formula:

$$P_a = 10\log\left[\left|S_{21}^{PORT1}\right|^2\left(\frac{\mathrm{Re}(Z_{SIS})}{R_{port}}\right)+\left|S_{21}^{PORT2}\right|^2\left(\frac{\mathrm{Re}(Z_{SIS})}{R_{port}}\right)\right] \quad (1)$$

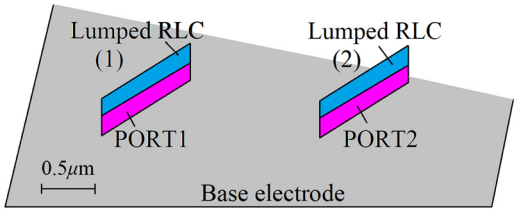


Fig. 2. The layout of the ports and boundary conditions corresponding to SIS junctions in Ansys HFSS simulation.

### B. Fabrication

The experimental samples were fabricated using the technological facilities "Cryointegral" at Kotelnikov Institute of Radio Engineering and Electronics of RAS [13-15]. The key processes are magnetron sputtering and optical lithography with using of masks prepared by means of electron-beam lithography. A high-ohmic silicon substrate is used for fabrication of the structures. An $Al_2O_3$ layer having a thickness of 100 nm is deposited as a buffer layer. Then, the base electrode made of NbTiN 325 nm thick is sputtered. This layer is etched over a resistive mask using plasma-chemical etching in $CF_4$. The next step is sputtering of a Nb/AlN/NbN (SIS) trilayer (80 nm/7 nm/80 nm thick) and its etching over a resistive mask right through to the NbTiN layer. The important point is to protect the sides of the SIS junctions and surface of NbTiN from the short connection with the upper electrode. Then, an insulator $SiO_2$ layer of transmission line 400 nm thick is deposited, which is also providing the isolating the SIS junction from the upper electrode. The upper electrode 500 nm thick made of Al is formed at final stage. Photo of the fabricated SIS junctions is shown in Fig.3.

## III. Results

### A. Experimental Setup

The cryogenic module with experimental sample is installed in the vacuum liquid helium cryostat with operating temperature of 4.2 K. We used the BWO as a powerful external source to pump the SIS detectors and to study the operational properties of the transmission lines. The photo of the experimental setup is shown in Fig. 4. The BWO unit has the frequency emission range of 0.94-1.1 THz that is tuned by the cathode voltage $V_c$ in the range from 4 kV to 6 kV, and is cooled by flowing water. To collect the output emission of the BWO at relatively narrow beam, a horn is used. The input window of the cryostat is made of Mylar that is almost transparent in THz range.

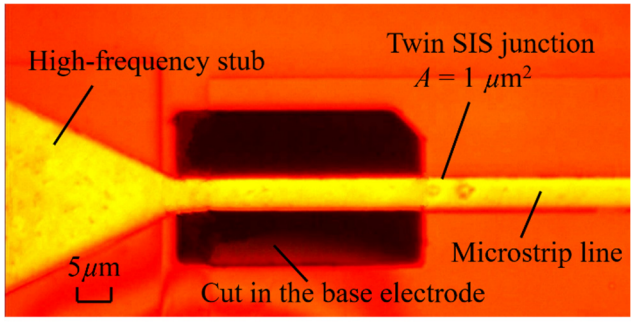


Fig. 3. Photo of the detecting section of integrated structure of design #1, twin SIS junction in the long section of microstrip line is presented.

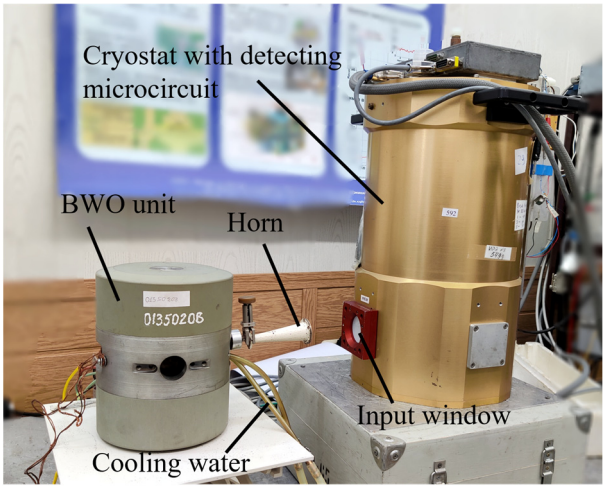


Fig. 4. Photo of the experimental setup for detecting THz signal from BWO by the SIS-based integrated circuit.

### B. Measurements

The high-frequency pumping of the SIS junctions was studied by measuring the current–voltage curves (IVCs). For precise dc measurements, a low-noise current source was used which is developed specifically for testing of the SIS junctions in a voltage-set operating mode, with typical voltages below 10 mV.

The IVCs of the SIS junctions embedded in microcircuit of design #1 are presented in Fig. 5, and for design #2 – in Fig. 6. In all graphs in Fig. 5 and Fig. 6 black solid curve indicates the "unpumped" IVC in the absence of the BWO signal, while the colored curves indicate the pumping of the SIS junctions at different BWO operating points, i.e. at different power and frequencies. Fig. 5(a) is related to the short microstrip section of design #1 (see the left branch in Fig. 1(a)), and Fig. 5(b) is related to the long section (see the right branch in Fig. 1(a)). As for design #2 utilizing the two symmetrical transmission lines with resonators, the result of one section, which is to the right in Fig. 1(b), is presented in Fig. 6. The maximum absorption power obtained in the experiment is shown by upper curves in both Figs. 5, 6. The BWO is a voltage-controlled oscillator with linear $V_c$ vs $f$ dependence; the unit with output frequency of 1.035 GHz at $V_c = 5$ kV and a tuning coefficient ~70.73 MHz/V was used. Thus, the SIS pumping was studied in the range from ~1.02 THz to ~1.1 THz. The BWO could operate also at frequencies down to 0.94 THz, but the power was too low and did not lead to changing the SIS IVC.

### C. Analysys

The pumping of the SIS junctions at THz frequencies leads to the two simultaneous tunneling effects: Shapiro current steps and quasiparticle current steps [4,5,16]. In our case, the SIS critical current was not suppressed, therefore the Shapiro steps can be clearly seen: the first one at a voltage of about 2.13-2.26 mV, corresponding to a frequency 1.03-1.09 THz according to Josephson constant of 483.6 GHz/mV, and the second one at the voltage of about 4.4 mV corresponding to the doubled pumping frequency. One can note that the steps voltage are in full agreement with the BWO output frequency: the higher oscillation frequency leads to higher voltage of the Shapiro step on the IVC.

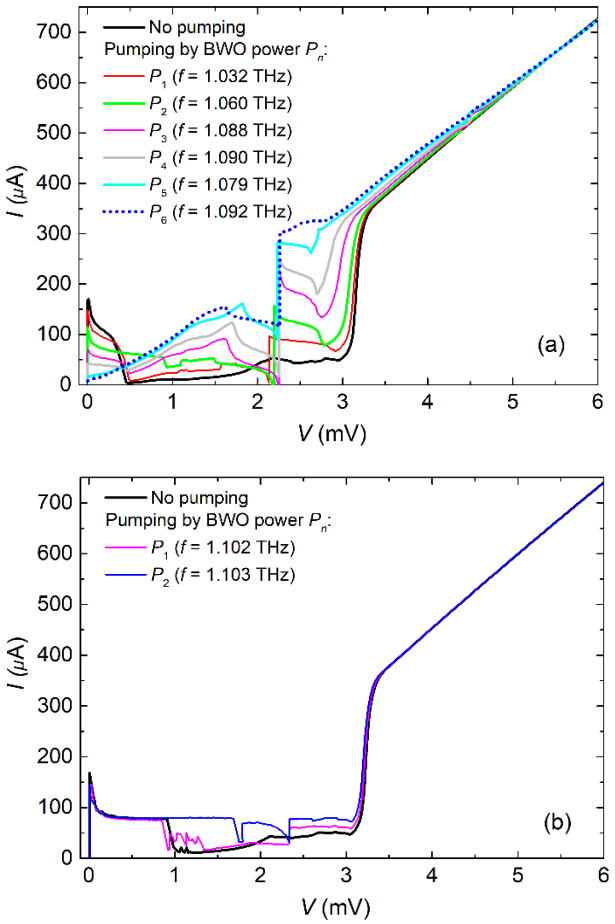


Fig. 5. The current-voltage curves of the twin SIS junction of desing #1 embedded (a) in the short mictrostrip section and (b) in the long microstrip section: black curve – IVC without signal from BWO; colored curves – pumping by BWO signal at different $V_c$ in the range between ~5 and ~6 kV. $R_n$ of the junction is 7.14 Ω for (a), and 6.86 Ω for (b).

The numerical results of design #1 for the power absorbed by twin SIS junctions in the two sections (short and long one, see Fig.1 a) are presented in Fig. 7a. The frequency of the maximum absorption is almost the same for both sections (about 0.93 THz), though they are distant by about 10 GHz.

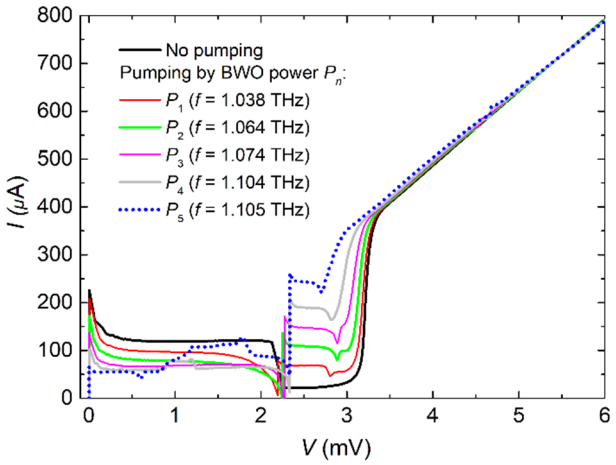


Fig. 6. The current-voltage curves of the twin SIS junction of design #2 embedded in one of the two symmetric mictrostrip sections with resonator: black curve – IVC without signal from BWO; colored curves – pumping by BWO signal at different $V_c$ in the range between ~5 and ~6 kV. $R_n$ of the junctions is 6.52 Ω.

At the same time, the absorption power $P_a$ in the long section is about 8 dB lower than in the short one at frequency about 1.1 THz (see dotted curve in Fig. 7a showing the difference in absorption power in the sections), which is in agreement with the experiment, where the maximum pumping current of the SIS in the long section (Fig. 5b) is much lower than that in the short one (Fig. 5a). One can note that the saturation of the SIS junction by the BWO signal was obtained in the short section (see dotted curve in Fig. 5a), which demonstrated rather strong pumping and efficient detection.

The numerical results of design #2 for the power absorbed by twin SIS junctions in each section with resonator (see Fig.1 b) are presented in Fig. 7b. Since the sections are identical, both the numerical and experimental results only for one section are presented. A strong pumping was also obtained for design #2 (see dotted curve in Fig. 5b), but did not lead to the saturation as it did for short section in design #1.

## IV. Conclusions

Integrated structures based on the SIS junctions can operate as high-sensitive receiving systems at frequencies above 1 THz, but fabrication and optimization of the superconducting transmission lines operating at such high frequencies is a difficult task. We developed, numerically simulated, fabricated and experimentally studied two designs of integrated circuits based on the Nb/AlN/NbN SIS junctions embedded in NbTiN/$SiO_2$/Al transmission lines. The BWO unit was used as the external THz source, and the slot antenna integrated to the silicon lens was utilized as a feeder. A strong pumping of the SIS junctions was obtained at frequency range 1.02-1.1 THz, demonstrating the successful operation of both the SIS junction and the transmission line.

## Acknowledgment

We thank Kirill Rudakov for assistance with numerical simulations and fruitful discussions. We acknowledge for access to equipment of the unique scientific unit “Cryointergral” (#352529), supported by the Ministry of Science and Higher Education of the Russian Federation (RF2296.61321X0041), which was used for study.

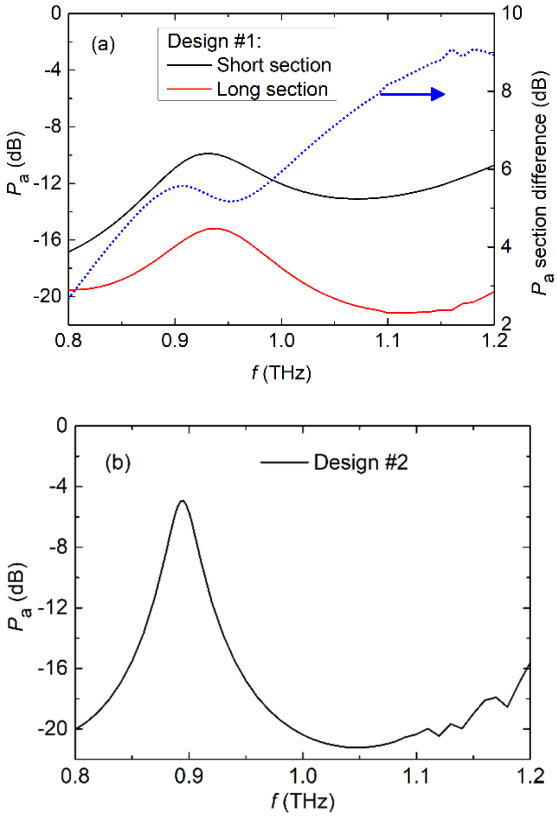


Fig. 7. Numerical results of absorbed power by the SIS junctions in two sections (a) for design #1 containing short and long sections, and (b) for design #2 with symmetrical sections including resonators.

## References

[1] S.L. Dexheimer, Terahertz Spectroscopy: Principles and Applications. CRC Press, New York, 2008, 360 p.

[2] D.F. Plusquellic, K. Siegrist, E.J. Heilweil, and O. Esenturk, "Applications of Terahertz Spectroscopy in Biosystems," ChemPhysChem, vol. 8, no. 17, pp.2412–2431, Nov. 2007.

[3] A.G. Davies, A.D.Burnett, W. Fan, E.H. Linfield, and J.E. Cunningham, "Terahertz spectroscopy of explosives and drugs," Mater. Today, vol. 11, no. 3, pp. 18–26, Mar. 2008.

[4] A. Barone and G. Paterno, Physics and Applications of the Josephson Effect. Hoboken, NJ, USA: Wiley, 1982.

[5] J.R. Tucker and M.J. Feldman, "Quantum detection at millimeter wavelengths," Rev. Mod. Phys., vol. 57, no. 4, pp. 1055–1113, Oct. 1985.

[6] A. Vettoliere et al., "High-Quality Ferromagnetic Josephson Junctions Based on Aluminum Electrodes," Nanomaterials, vol. 12, no. 23, p. 4155, Nov. 2022.

[7] D.C. Mattis and J. Bardeen, “Theory of the Anomalous Skin Effect in Normal and Superconducting Metals,” Physical Review, vol. 111, no. 2, pp. 412-417, Jul. 1958.

[8] J.W. Kooi et al., "Low-Loss NbTiN Films for THz SIS Mixer Tuning Circuits," International Journal of Infrared and Millimeter Waves, vol. 19, no. 3, pp. 373–383, Mar. 1998.

[9] B.D. Jackson et al., "NbTiN/$SiO_2$/Al Tuning Circuits For Low-Noise 1 THz SIS mixers," vol. 11, no. 1, pp. 653-656, Mar. 2001.

[10] A.R. Kerr and S. K. Pan, "Some recent developments in the design of SIS mixers," International journal of infrared and millimeter waves, vol. 11, no, 10, pp. 1169-1187, Oct. 1990.

[11] V. Belitsky, C. Risacher, M. Pantaleev, and V. Vassilev, "Superconducting Microstrip Line Model Studies at Millimetre and Sub-Millimetre Waves," International journal of infrared and millimeter waves, vol. 27, no. 1, pp. 809-834. Feb. 2006.

[12] A. Khudchenko et al., "Dispersive Spectrometry At Terahertz Frequencies for Probing the Quality of NbTiN Superconducting Films," IEEE Trans. on Appl. Supercond., vol. 32, no. 4, p. 1500506, Jun. 2022.

[13] P.N. Dmitriev et al., “High Quality Nb-based Integrated Circuits for High Frequency and Digital Applications,” IEEE Trans. on Appl. Supercond., vol. 13, no. 2, pp. 107–110, Jun. 2003

[14] A. Khudchenko et al., "High-Gap Nb-AlN-NbN SIS Junctions for Frequency Band 790–950 GHz," IEEE Trans. Terahertz Sci. Technol., vol. 6, no. 1, pp. 127–132, Dec. 2016.

[15] A.M. Chekushkin, L.V. Filippenko, V.V. Kashin, M.Yu. Fominskiy, and V.P. Koshelets, "Investigation of Thin Films for Fabrication of Nb/Aln/Nbn Tunnel Junctions and Microstrip Lines Of NbTiN-$SiO_2$-Al," RENSIT: Radioelectronics. Nanosystems. Information technologies, vol. 13, no. 4, pp. 419-426, Nov. 2017.

[16] C.C. Grimes and S. Shapiro, "Millimeter-Wave Mixing with Joseyhson Junctions," Physical Review, vol. 169, no. 2, pp. 397-406, May 1968.